

Dalton Transactions

Accepted Manuscript



This is an *Accepted Manuscript*, which has been through the Royal Society of Chemistry peer review process and has been accepted for publication.

Accepted Manuscripts are published online shortly after acceptance, before technical editing, formatting and proof reading. Using this free service, authors can make their results available to the community, in citable form, before we publish the edited article. We will replace this *Accepted Manuscript* with the edited and formatted *Advance Article* as soon as it is available.

You can find more information about *Accepted Manuscripts* in the [Information for Authors](#).

Please note that technical editing may introduce minor changes to the text and/or graphics, which may alter content. The journal's standard [Terms & Conditions](#) and the [Ethical guidelines](#) still apply. In no event shall the Royal Society of Chemistry be held responsible for any errors or omissions in this *Accepted Manuscript* or any consequences arising from the use of any information it contains.

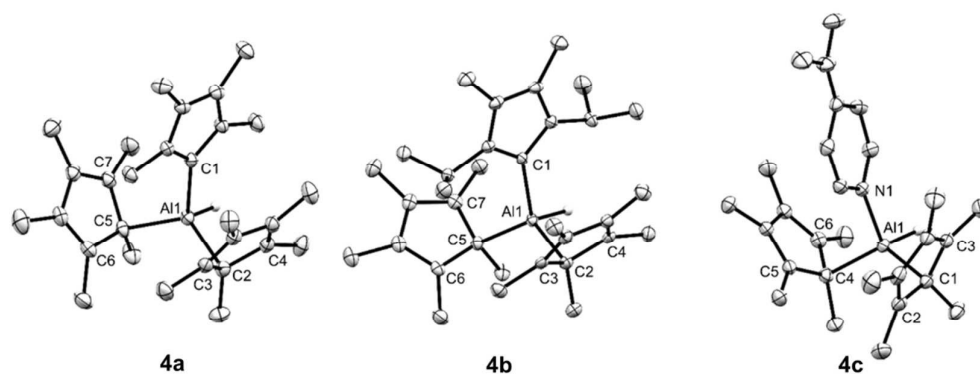
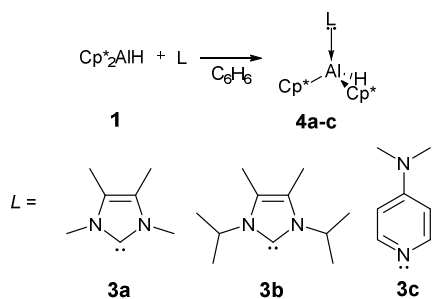


Figure 1 X-Ray crystal structures of NHC coordinated adducts of **1**. Thermal ellipsoids at 50% probability and hydrogen atoms (except Al-H) omitted for clarity. Selected bond distances (Å): **4a**: Al1-C1 2.0571(15), Al1-C2 2.0857(16), Al1-C3 = 2.65437(8), Al1-C4 = 2.79902(7), Al1-C5 2.0901(15), Al1-C6 3.03754(10), Al1-C7 2.70808(8); **4b**: Al1-C1 2.069(2), Al1-C2 2.082(2), Al1-C3 2.7948(3), Al1-C4 2.92435(18), Al1-C5 2.072(2), Al1-C6 3.1378(2), Al1-C7 2.8882(3); **4c**: Al1-N1 1.943(2), Al1-C1 2.081(3), Al1-C2 2.70138(8), Al1-C3 2.92094(8), Al1-C4 2.067(3), Al1-C5 2.81996(7), Al1-C6 2.66689(18).



Scheme 2 Synthesis of base coordinated adducts of Cp^*_2AlH

With the diverse effects of Lewis bases on reductive elimination from silicon and tin centres, we were interested in how Lewis bases would interact with the reductive elimination chemistry of Cp^*_2AlH , **1**. Treatment of Cp^*_2AlH with N-heterocyclic carbenes (**3a**, 1,3,4,5-tetramethylimidazol-2-ylidene; **3b**, 1,3-diisopropyl-4,5-dimethylimidazol-2-ylidene) or dimethyl aminopyridine (DMAP) results in the formation of 4-coordinate aluminium adducts **4a-c** in high yields.[†] No reaction was observed between **1** and the bulky NHC IPr (IPr = $\text{C}\{\text{N}(2,6\text{-iPr}_2\text{C}_6\text{H}_3)\text{CH}\}_2$),²² probably due to steric factors.

The coordination of the NHC ligands **3a** or **3b** to Cp^*_2AlH **1** was readily apparent in the ^1H NMR spectra of **4a** and **4b**. A dative Al-C interaction is confirmed by new signals observed for the now inequivalent methyl or isopropyl C-H groups of the NHC ligands (**4a** δ = 1.29 and 1.15 ppm; **4b** δ = 6.08 and 3.76 ppm), which also display the expected downfield shifts observed for coordinated NHC ligands.²³ The typical upfield shift of NHC donor carbon resonances upon coordination could not be confirmed because these signals were not observable for **4a** or **4b**, likely because of line broadening due to quadrupolar ^{27}Al . The chemical shift of the Cp^* methyl groups is only slightly perturbed by coordination of the NHC ligands (**4a** δ = 1.98 ppm; **4b** δ = 2.06 ppm; **1** δ = 1.91 ppm) and remains a lone singlet, indicating rapid sigmatropic shifts of the cyclopentadienyl substituents.^{24,25}

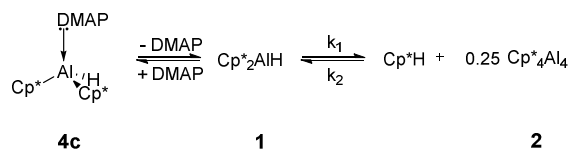
Coordination of the DMAP ligand in the adduct **4c** is confirmed by the observation of two upfield-shifted signals (δ

= 7.52 $^3J_{\text{H-H}}$ = 6.0 Hz; δ = 5.59 $^3J_{\text{H-H}}$ = 7.0 Hz) for the aromatic protons of the DMAP ligand.

X-Ray diffraction of single crystals of **4a-c** confirm our NMR spectroscopic assignments. All compounds possess the expected tetrahedral aluminium centre, with both of the Cp^* substituents η^1 coordinated (Figure 1). The long C-Al distances for the alkene ring carbons of the Cp^* substituents in **4a-c** preclude any Al-C bonding interactions. This differs from the reported structure of **1**, where the two Cp^* rings are η^2 and η^3 coordinated.²¹ Clearly, the coordination of strong σ -donor to the aluminium centre of **1** is favoured over the weaker donation of electron density from the π -system of the Cp^* ligands. Compound **4a** is isostructural with its gallium analogue,²⁶ and the NHC bond distances in **4a** and **4b** are directly comparable to the very few reported NHC adducts of aluminium.^{27,28}

In contrast to the group 14 systems mentioned previously, the interaction of Lewis bases with the aluminium hydride **1** does not result in reductive elimination reactivity. Even after heating the NHC adducts **4a** or **4b** at 100 °C for several days, no elimination of Cp^*H was observed.²⁹ However, heating solutions of the DMAP adduct **4c** at 80 °C resulted in reductive elimination of Cp^*H and formation of tetramer **2** as the only aluminium-containing product, along with uncoordinated DMAP. The rate of Cp^*H elimination from **4c** is significantly slower than that from Cp^*_2AlH **1** (for example, after 100 minutes at 353 K, 31.3 % of **4c** was converted to the tetramer **2** whilst 90.7 % of **1** had been converted).

In order to explain our observations, we propose a mechanism involving the reversible dissociation of DMAP from the adduct **4c** under the reaction conditions. Reductive elimination to form **2** can only take place from **1**; the DMAP adduct **4c** does not itself eliminate Cp^*H (scheme 3). The



Scheme 3 Reversible coordination of DMAP to **1**

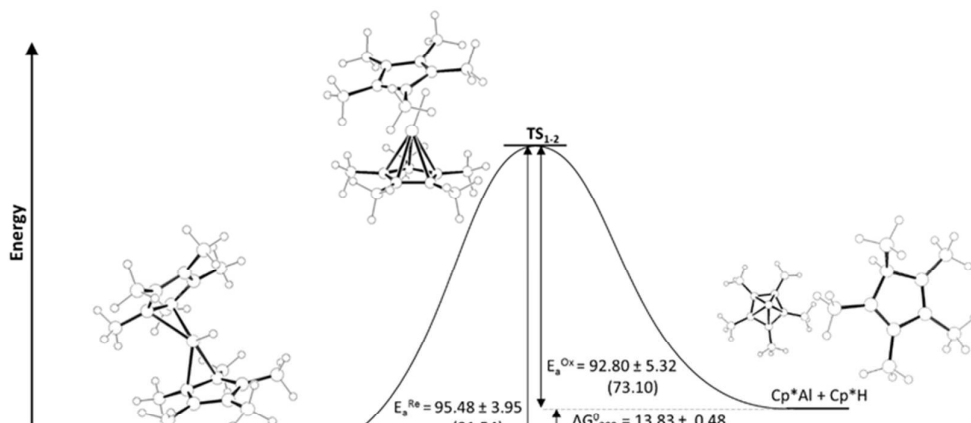


Figure 2 Potential energy diagram with energies (theoretical) stated in kJ mol⁻¹. Calculated energies predicated at the BP86/def-TZVPP level of theory using the BP86/def2-SVP optimised geometries (shown).

formation of (Cp*Al)₄ is not observed when the NHC adducts **4a** and **4b** are heated because of the stronger coordination of these ligands to the aluminium centre.

The proposed reversible coordination of DMAP to **1** at higher temperatures is supported by the observation of time-averaged chemical shifts for the DMAP aromatic CH protons. For example, when a sample of **4c** in d₈-toluene is heated to 363K, broad resonances are observed in the ¹H NMR spectrum at δ = 7.71 and 5.88 (at 300K: **4c** δ = 7.52, 5.59; DMAP δ = 8.44, 6.10). Monitoring the rate of reductive elimination of Cp*H from Cp*₂AlH **1** and from **4c** confirms that DMAP inhibits Cp*H elimination. Upon heating a solution of **1** for 150 minutes, equilibrium was reached with 95.9 % conversion to **2** and Cp*H. However, at equilibrium solutions of **4c** only displayed 35.9 % conversion to **2**.

Why does base coordination to **1** inhibit reductive elimination, when in other main-group systems reductive elimination can be promoted by the coordination of donor ligands? We sought to understand this observation by undertaking a mechanistic study of reductive elimination from **1**.

We initially confirmed Fischer's report²¹ that reductive elimination of Cp*H from the hydride **1** is reversible, and determined equilibrium constants for this process. Monitoring a d₈-toluene solution of **1** by ¹H NMR spectroscopy reveals 100 % conversion to **2** and Cp*H at 100 °C; upon cooling to 70 °C and then to 28 °C, compound **1** was cleanly regenerated and the conversion to **2** fell to 91.3 and 88.5 % respectively (Figures S9, S11). By measuring the concentrations of (Cp*Al)₄, **2**, Cp*₂AlH **1** and Cp*H we determined K_{eq} for the equilibrium depicted in scheme 1 at a range of temperatures (Table S3). We were thus able to determine ΔG⁰₃₀₀ as +13.83 ± 0.48 kJ mol⁻¹, indicating reductive elimination from **1** to **2** is an endothermic process, as might be expected for the reduction of Al^{III} to Al^I.³⁰

Having established experimental values for thermodynamic parameters of Cp*H reductive elimination, we studied the kinetics of this reaction. An important assumption we make is that the tetramerisation of Cp*Al to (Cp*Al)₄, and the reverse

process, proceeds with lower barriers than reductive elimination of oxidative addition of Cp*H. The tetramerisation energy for Cp*Al has been measured experimentally as 150 ± 20 kJ mol⁻¹, and tetramer and monomer are in rapid equilibrium under our reaction conditions.³¹

Oxidative addition of Cp*H to Cp*Al is significantly faster than reductive elimination from **1**; fitting our experimental data to the model in Scheme 1 we determined rate constants k₁ and k₂ at 333 K as 1.46 × 10⁻³ ± 0.04 × 10⁻³ s⁻¹ and 35 × 10⁻³ ± 4 × 10⁻³ M⁻¹ s⁻¹ respectively. An Eyring plot (figure S13) reveals an activation barrier of 95.48 ± 3.95 kJ mol⁻¹ for reductive elimination (E_a^{RE}) of Cp*H from **1**. We could only obtain rate data for oxidative addition of Cp*H to Cp*Al at a limited range of temperatures, so are unable to accurately determine a value for the activation barrier of this reaction. However, E_a^{OA} can be estimated by subtracting ΔG⁰₃₀₀ for reaction 1 from E_a^{RE} giving a value of 81.65 ± 3.97 kJ mol⁻¹. This value correlates well with the value we estimated from an Eyring plot with limited rate data (figure S14) which was 92.80 ± 5.32 kJ mol⁻¹. Unexpectedly, the entropy of activation for reductive elimination is close to zero, and slightly negative, at -0.167 ± 2.64 J K⁻¹ mol⁻¹, rather than the positive figure that could be expected for a reductive elimination reaction.

Although coordination of an external Lewis base to **1** does not promote reductive elimination of Cp*H, we questioned if one of the Cp* ligands of **1** could play this role, particularly since X-ray crystallography reveals that the two Cp* ligands of **1** adopt η² and η³ coordination modes.²¹ A shift to higher hapticity of one Cp* ligand could explain the slightly negative entropy of activation for reductive elimination. An alternative explanation could be an ionic-type mechanism involving the dissociation of a Cp*⁻ ligand to form a transient [Cp*AlH]⁺ species, with solvent ordering around the charged intermediates being responsible for the negative entropy of activation.³² We examined the reductive elimination of Cp*H from Cp*₂AlH using DFT (figure 2) in order to better understand the mechanism.

Geometry optimisations were performed for compounds **1**, **2**, and Cp*H and the transition state that links them (geometries were optimised at the BP86/def2-SVP level of

theory, and confirmed as minima by frequency calculations (ref to SI). The transition state for reductive elimination of Cp*H from **1**, TS₁₋₂ was identified by a transition state search at the BP86/def2-SVP level of theory. Energies were calculated at the BP86/def2-TZVPP level of theory. The calculated geometries of **1** and **2**, are consistent with experimental observations, and predicted ΔG_{300}^0 and activation barriers for reductive elimination of Cp*H from **1** are in excellent agreement with those determined experimentally ($\Delta G_{300}^0 = +18.44$ vs $+13.83 \pm 0.48$ kJ mol⁻¹; $E_a^{RE} = 91.54$ vs 95.48 ± 3.95 kJ mol⁻¹).

The geometry of TS₁₋₂ is informative in explaining why base coordination to **1** inhibits reductive elimination of Cp*H. In TS₁₋₂, one Cp* ligand is η^5 with C-Al distances essentially identical to those in Cp*Al (average C-Al distance for η^5 Cp* in TS₁₋₂ = 2.358 Å; Cp*Al = 2.355 Å). This interaction can not take place whilst an external Lewis base is coordinated.

Although the geometry around the departing Cp*(H) ring is planar in TS₁₋₂, there is a clear interaction between a Cp* ring carbon and the Al-H functionality, with a C-H distance (1.461 Å) almost suggestive of a deprotonation of a Cp*AlH⁺ species by Cp*⁻. The calculated Al-H bond distance increases dramatically from **1** to TS₁₋₂ (1.579 to 1.837 Å). Consistent with this, when NPA charges on the Al-H were compared, a substantial depletion of negative charge at the hydride was observed when moving from **1** to TS₁₋₂ (from -0.373 to -0.049). Notably, TS₁₋₂ is very similar to that very recently calculated by Cao and Zhang for the oxidative addition of Cp*H to Roesky's NacNacAl^I compound (NacNac = HC[CMeN(2,6-ⁱPr₂-C₆H₃)]₂).³³

We conclude that Cp*Al, like NacNacAl^I, activates acidic C-H bonds *via* an initial proton transfer from C-H to the aluminium(I) centre. Ligand effects are important: ΔG_{298}^0 for oxidative addition of Cp*H to NacNacAl^I (calculated by Cao and Zhang to be -100.9 – -108.0 kJ mol⁻¹) is significantly higher than that for Cp*Al (ΔG_{300}^0 measured by us to be -13.83 ± 0.48 kJ mol⁻¹). Thus, it seems that Cp* can stabilise Al^I more effectively than the NacNac ligand; the aromatisation of the η^5 Cp* ligand in **2** almost certainly offsets the thermodynamically unfavourable transformation from Al^{III} to Al^I. In the same way, the aromatisation of the Cp* ligand in TS₁₋₂ lowers the barrier to reductive elimination of Cp*H (which we estimate at 80-90 kJ mol⁻¹) compared to the calculated value for NacNacAl^I (167 – 188 kJ mol⁻¹), rendering the oxidative addition of Cp*H to Cp*Al reversible, when that to NacNacAl^I is not. As might be expected, the coordination of strong σ -donors to the aluminium centre of **1** inhibits reductive elimination. This effect is twofold in origin. Firstly, the presence of a strong electron donor substantially stabilises the high(er) oxidation state aluminium centre. Secondly, coordination inhibits the aromatisation of the Cp* ligands required to enable reductive elimination. The combined effects of the π -donating Cp* ligands and the coordination of strong σ -donors in modulating the Al^{III}/Al^I process is similar to the recently reported effect of strong σ -donors in oxidative addition to germylenes.³⁴ Such ligands not only enable oxidative addition reactivity by narrowing the HOMO/LUMO gap in the low-valent species, but

also favour the low oxidation state species by providing increased electron density.

Continued study of reaction mechanisms of (reversible) oxidative addition and reductive elimination in low-valent main-group systems will be essential in developing effective principles for ligand design.

The authors would like to thank the European Commission, the EPSRC and the University of Edinburgh for financial support. This work was supported by a career integration grant, funded by the FP7 Marie Curie Actions of the European Commission (PCIG14-GA-2013-631483). MJC would like to thank Prof. Polly Arnold for helpful discussions.

Notes and references

‡ For full experimental, spectroscopic and computational details, please refer to the ESI.

- 1 R. H. Crabtree, *The Organometallic Chemistry of the Transition Metals*, John Wiley & Sons Ltd, 6th Edn., 2014.
- 2 P. P. Power, *Nature*, 2010, **463**, 171–177.
- 3 G. H. Spikes, J. C. Fettinger and P. P. Power, *J. Am. Chem. Soc.*, 2005, **127**, 12232–12233.
- 4 G. D. Frey, V. Lavallo, B. Donnadieu, W. W. Schoeller and G. Bertrand, *Science*, 2007, **316**, 439–442.
- 5 Y. Peng, M. Brynda, B. D. Ellis, J. C. Fettinger, E. Rivard and P. P. Power, *Chem. Commun.*, 2008, 6042–6044.
- 6 Y. Peng, J. Guo, B. D. Ellis, Z. Zhu, J. C. Fettinger, S. Nagase and P. P. Power, *J. Am. Chem. Soc.*, 2009, **131**, 16272–16282.
- 7 J. Li, C. Schenk, C. Goedecke, G. Frenking and C. Jones, *J. Am. Chem. Soc.*, 2011, **133**, 18622–18625.
- 8 L. Zhao, F. Huang, G. Lu, Z. Wang and P. V. R. Schleyer, *J. Am. Chem. Soc.*, 2012, **134**, 8856–8868.
- 9 T. J. Hadlington, M. Hermann, J. Li, G. Frenking and C. Jones, *Angew. Chem. Int. Ed.*, 2013, **52**, 10199–10203.
- 10 A. V. Protchenko, J. I. Bates, L. M. a Saleh, M. P. Blake, A. D. Schwarz, E. L. Kolychev, A. L. Thompson, C. Jones, P. Mountford and S. Aldridge, *J. Am. Chem. Soc.*, 2016, **138**, 4555–64.
- 11 A. J. Arduengo, C. A. Stewart, F. Davidson, D. A. Dixon, J. Y. Becker, B. S. A. Culley and M. B. Mizzen, *J. Am. Chem. Soc.*, 1987, **109**, 627–647.
- 12 S. M. McCarthy, Y. Lin, D. Devarajan, J. W. Chang, H. P. Yennawar, R. M. Rioux, D. H. Ess and A. T. Radosevich, *J. Am. Chem. Soc.*, 2014, **136**, 4640–4650.
- 13 T. P. Robinson, D. M. De Rosa, S. Aldridge and J. M. Goicoechea, *Angew. Chem. Int. Ed.*, 2015, **54**, 13758–13763.
- 14 A. Pal and K. Vanka, *Inorg. Chem.*, 2016, **55**, 558–565.
- 15 G. Zeng, S. Maeda, T. Taketsugu and S. Sakaki, *Angew. Chem. Int. Ed.*, 2014, **53**, 4633–4637.
- 16 D. Kummer and H. Koester, *Angew. Chem. Int. Ed.*, 1969, **8**, 878–879.
- 17 F. Meyer-Wegner, A. Nadj, M. Bolte, N. Auner, M. Wagner, M. C. Holthausen and H.-W. Lerner, *Chemistry*, 2011, **17**, 4715–9.
- 18 C. P. Sindlinger, A. Stasch, H. F. Bettinger and L. Wesemann, *Chem. Sci.*, 2015, **6**, 4737–4751.
- 19 D. W. Stephan, *J. Am. Chem. Soc.*, 2015, **137**, 10018–10032.
- 20 T. Chu, I. Korobkov and G. I. Nikonov, *J. Am. Chem. Soc.*, 2014, **136**, 9195–9202.
- 21 C. Ganesamoorthy, S. Loerke, C. Gemel, P. Jerabek, M. Winter, G. Frenking and R. Fischer, *Chem. Commun.*, 2013, **49**, 2858–2860.
- 22 L. Jafarpour, E. D. Stevens and S. P. Nolan, *J. Organomet. Chem.*, 2000, **606**, 49–54.
- 23 X. Li, J. Su and G. H. Robinson, *Chem. Commun.*, 1996, 2683–2684.
- 24 P. Jutzi, *Adv. Organomet. Chem.*, 1986, 217–295.
- 25 P. Jutzi, *Chem. Rev.*, 1986, **86**, 983–996.

Journal Name

COMMUNICATION

- 26 J. D. Gorden, C. L. B. Macdonald, and A. H. Cowley, *J. Organomet. Chem.*, 2002, **643-644**, 487–489.
- 27 J. M. Pietryga, J. D. Gorden, C. L. B. Macdonald, A. Voigt, R. J. Wiacek, and A. H. Cowley, *J. Am. Chem. Soc.*, 2001, **123**, 7713–7714.
- 28 M. Wu, M. A. M. Gill, Lu Yunpeng, L. Falivene, Li Yongxin, R. Ganguly, L. Cavallo, and Felipe García, *Dalton Trans.*, 2015, **44**, 15166.
- 29 When we attempted treating $(Cp^*Al)_4$ with NHCs to directly synthesise base-coordinated aluminium(I) species $Cp^*Al.NHC$, we also observed no reaction.
- 30 This differs from the findings of Fischer in reference 21, who reports (on the basis of DFT calculations) that this reaction is slightly exergonic.
- 31 J. Gauss, U. Schneider, R. Ahlrichs, C. Dohmeier and H. Schnöckel, *J. Am. Chem. Soc.*, 1993, **115**, 2402–2408.
- 32 P. K. Byers, A. J. Canty, M. Crespo, R. J. Puddephatt and J. D. Scott, *Organometallics*, 1988, **7**, 1363–1367.
- 33 X. Zhang and Z. Cao, *Dalton Trans.*, 2016, **45**, 10355–10365.
- 34 M. Usher, A. V. Protchenko, A. Rit, J. Campos, E. L. Kolychev, R. Tirfoin, S. Aldridge, *Chem. Eur. J.*, 2016, **22**, 11685.